WEP Warwick Evans Publishing

International Journal of Natural Resources and Environmental Studies

ISSN: 3006-2012 (Print), ISSN: 3006-0834 (Online) | Volume 2, Number 3, Year 2024
DOI: https://doi.org/10.62051/ijnres.v2n3.01
Journal homepage: https://wepub.org/index.php/IJNRES/index

# Pore Size Distribution and Pore Connectivity Response Characteristics of Anthracite Injected with Carbon Dioxide in Different Phases

Jiale Yi

School of Resources & Environment, Henan Polytechnic University, Jiaozuo 454000, China

## ABSTRACT

The adsorption of $CO_2$ changes the pore content in coal. After $CO_2$ adsorption, pore content in coal shows a trend of first increasing, then decreasing and then increasing. $CO_2$ adsorption pressure, $CO_2$ adsorption time and $CO_2$-$H_2O$ slightly change the variation range of pore size, but the trend remains unchanged. For example, in the case of $CO_2$ adsorption for 72 hours, the pore content of 2~10nm and >700nm is generally increased, and the pore content of 10~700nm is significantly reduced. In the case of 144 hours of $CO_2$ adsorption, the pore content of 2~20nm and >700nm generally increased, and the pore content of 20~700nm significantly decreased. When water +$CO_2$ was adsorbed for 144 hours, the pore content of 2~12nm and >700nm generally increased, and the pore content of 12~700nm generally decreased. The coal samples show a certain lag of mercury removal before and after $CO_2$, which indicates that there are some ineffective pores in the coal. The mercury removal efficiency of the coal sample after $CO_2$ adsorption is generally lower than that of the dry sample, indicating that a large number of inefficiently connected pores are generated after $CO_2$ adsorption. That is, $CO_2$ does increase a large number of pores in coal, but the pores are mainly non-connected pores, that is, $CO_2$ has a weak improvement in the connectivity of the pores in coal.

## KEYWORDS

Pore content; Mercury removal efficiency; Disconnected pore.

## 1. INTRODUCTION

Fractures, as key conduits for fluid transport and production in coal reservoirs, have a decisive impact on reservoir permeability. Fracture development is generally divided into macroscopic and microscopic levels, with microscopic fractures further classified into endogenous and exogenous types. It is widely believed that fractures are the result of internal forces, external forces, or a combination of both, with tectonic evolution, coal metamorphism, and coal rock composition playing crucial roles in their development. Yao et al. innovatively developed a fracture-matrix permeability model that correlates permeability with strain, considering the complete coupling between gas flow in the coal matrix and coal deformation, thereby providing a novel theoretical tool for predicting $CO_2$ injection into coal seams [1].

With the continuous advancement of physical testing techniques for coal pores and fractures, several important achievements have been made [2-4]. Scholars have extensively discussed the effects of CT on coal and supercritical $CO_2$ on enhancing permeability of coal reservoirs [5], and based on this, have preliminarily established methods for digital rock reconstruction of coal. Some researchers have begun to use AFM technology to study the nanoscale structure of coal and conducted preliminary three-dimensional quantitative analysis of nanoscale pore structure parameters [6]. The emergence of

FIB-SEM technology has provided a new pathway for studying nanoscale pore structures, enabling the precise reproduction of three-dimensional structural details of pores in coal samples.

# 2. SAMPLE AND METHODS

## 2.1. Sample collection and preparation

The samples used in the experimental research of this paper were taken from the Datong Mine No. 3 coal mine in Gaoping City, Shanxi Province, China. These coal samples were all taken from adjacent positions of the same large block. To ensure the accuracy and reliability of the experiments, three small pieces of original samples were randomly placed in sealed bags. The reflectance of vitrinite and microcomponents were tested using the Axio Scope.A1 multifunctional microscope produced by ZEISS company. The experimental conditions were room temperature at 23°C and humidity at 60%. The tests were conducted according to the recommended standards of the petroleum industry SY/T 5124-2012 and SY/T 5124-1995. Table 1 shows the test results of this experiment. The results indicate that the random average reflectance of vitrinite is 2.34%, 2.29%, and 2.16% respectively, indicating high-rank coal. Microcomponent analysis shows that these samples are predominantly vitrinite, accounting for 97.5%, 96.0%, and 97.3% respectively, with some inertinite, accounting for 2.5%, 4.0%, and 2.7% respectively. The total organic matter accounts for 93.1%, 95.4%, and 96.3% respectively, pyrite accounts for 0.1% in all cases, and other minerals account for 6.8%, 4.5%, and 3.6% respectively.

**Table 1.** Basic information of the coal samples.

| Sample source | Total rock (%) | | | maceral (%) | | | Vitrinite reflectance (%) | | |
|---|---|---|---|---|---|---|---|---|---|
| | Total organic matter | Pyrite | Other minerals | Liptinite | Vitrinite | Inertinite | Min | Max | Average value |
| The 3# coal of Datong Mine | 93.1 | 0.1 | 6.8 | / | 97.5 | 2.5 | 2.11 | 2.51 | 2.34 |
| | 95.4 | 0.1 | 4.5 | / | 96.0 | 4.0 | 2.21 | 2.45 | 2.29 |
| | 96.3 | 0.1 | 3.6 | / | 97.3 | 2.7 | 1.99 | 2.35 | 2.16 |

## 2.2. Water injection and gas injection experiments

**Table 2.** Experimental conditions for coal powder.

| Coal sample identification number | Experimental temperature (°C) | Moisture condition | Gas injection type | Gas injection time (h) | Gas injection pressure (MPa) |
|---|---|---|---|---|---|
| 1 | 40 | Dry | / | / | / |
| 2 | | Dry | $CO_2$ | 72h | 4MPa |
| 3 | | Dry | $CO_2$ | 72h | 6MPa |
| 4 | | Dry | $CO_2$ | 72h | 8MPa |
| 5 | | Dry | $CO_2$ | 144h | 4MPa |
| 6 | | Dry | $CO_2$ | 144h | 6MPa |
| 7 | | Dry | $CO_2$ | 144h | 8MPa |
| 8 | | Immersion water | $CO_2$ | 144h | 4MPa |
| 9 | | Immersion water | $CO_2$ | 144h | 6MPa |
| 10 | | Immersion water | $CO_2$ | 144h | 8MPa |

All samples in the experimental procedure were subjected to 24 hours of drying at 105°C in an oven to remove all moisture before conducting the triaxial experiments. Then, according to the experimental plan, the samples were prepared under the corresponding $CO_2$ pressure. After the

pressure gauge readings stabilized, continuous $CO_2$ injection was carried out for 3 days and 6 days at the given pressure and temperature. Studies have shown that the structure of coal still undergoes slow changes even after one year of $CO_2$ injection, but the main interaction between coal and $CO_2$ is completed within the first few days. Therefore, considering the timeliness of $CO_2$ adsorption, this study adopted continuous injection times of 3 days and 6 days.

### 2.3. Low-temperature N2 adsorption experiment

The low-temperature nitrogen adsorption experiment was conducted using the ASAP 2460 multi-station automatic surface area and pore size analyzer manufactured by Micromeritics Instrument Corporation in the United States, following the international standards ISO 15901-2:2006 and ISO 15901-3:2007. The sample used in the experiment was coal powder with a particle size of 0.18-0.25 mm. Nitrogen was used as the adsorption medium, with the analysis bath temperature set at -195.85°C and the relative pressure range from 0.005 to 0.996. In the analysis of nitrogen adsorption data, the multi-layer adsorption model proposed by Brumauer-Emmett-Teller (BET) was used to calculate the specific surface area, and the Barrett-Joyner-Halenda (BJH) equation was used to determine the pore size. The BET model is a widely used theoretical tool for calculating adsorption isotherms, suitable for studying the adsorption behavior of adsorbent surfaces in gases or solutions.

### 2.4. High-pressure mercury experiment.

The mercury intrusion porosimetry test gradually injects liquid mercury into the pores under external pressure. Smaller pore sizes require higher pressure to be filled. The experiment utilized the AutoPore IV 9520 fully automatic mercury porosimeter from Micromeritics Instrument Company, USA, following the international standard ISO 15901-1:2005. The coal sample used in the experiment was small coal blocks with a volume of about 3-4 $cm^3$. During the experiment, the injection pressure of mercury ranged from 0.0099 MPa to 413.46 MPa. The measurement lower limit was 5 nm, employing a computer-program-controlled point-by-point measurement method, and the samples were dried for 24 hours before the experiment. The pore size calculation employed the Washburn equation, with a surface tension of mercury set at 0.48 N/m and a contact angle between mercury and coal set at 140°.

## 3. RESULTS AND DISCUSSION

### 3.1. Changing characteristics of pore diameter distribution of coal

There are many ways to characterize the pore distribution characteristics of coal samples. Based on the data of low-temperature $N_2$ adsorption experiment and high-pressure mercury injection experiment, the pore volume change rate within the pore size range can be expressed by using the logarithmic form, and the curve amplitude is more obvious and intuitive. In this study, the differential of log pore volume to pore diameter is calculated, and the pore diameter distribution map of coal sample is drawn.

The pore size distribution results obtained by low temperature liquid nitrogen adsorption test and high pressure mercury injection test of coal samples under different $CO_2$ adsorption pressures are shown in Fig. 1 and Fig. 2. It can be seen from the pore size distribution diagram of low-temperature nitrogen test that under the condition of $CO_2$ adsorption for 72 hours, the pore content between 2 and 10nm is generally higher than that of the untreated original, but the pore content between 10 and 50nm is significantly smaller than that of the original, and the pore size distribution does not show regularity with the increase of $CO_2$ adsorption pressure. It can be seen from the pore size distribution diagram of high-pressure mercury injection test that under the condition of $CO_2$ adsorption for 72 hours, the pore content between 20 and 700nm is generally lower than the original pore content, while the pore content of >700nm is significantly increased and generally larger than the original pore content.

However, the increase of $CO_2$ adsorption pressure still has no regularity in pore size distribution. Therefore, combined with the results of the two experiments, it can be found that under the condition of $CO_2$ adsorption for 72 hours, the pore content of 2~10nm and >700nm generally increases, while the pore content of 10~700nm significantly decreases. The increase of $CO_2$ adsorption pressure has no regularity in the pore size distribution. It can be seen from the pore size distribution diagram of low-temperature nitrogen test that under the condition of 144 hours of $CO_2$ adsorption, the pore content between 2 and 20nm is generally larger than the original, and the pore content between 20 and 50nm is generally smaller than the original, and there is no obvious regularity. It can be seen from the pore size distribution diagram of high-pressure mercury injection test that the pore content between 20 and 700nm is generally lower than that of the original, while the pore content of >700nm increases significantly and is generally larger than that of the original. However, the pore size distribution is still irregular with the increase of $CO_2$ adsorption pressure. Therefore, combined with the results of the two experiments, it can be found that under the condition of 144 hours of $CO_2$ adsorption, the pore content of 2~20nm and >700nm generally increases, while the pore content of 20~700nm significantly decreases. The increase of $CO_2$ adsorption pressure has no regularity in the pore size distribution. It can be seen from the pore size distribution diagram of low-temperature nitrogen test that when water +$CO_2$ is adsorbed for 144 hours, the pore content between 2 and 12nm is generally larger than the original, and between 12 and 50nm is generally smaller than the original. It can be seen from the pore size distribution diagram of high-pressure mercury injection test that when water +$CO_2$ is adsorbated for 144 hours, the pore content between 20 and 700nm is generally lower than the original, while the pore content of >700nm is significantly increased, and is generally larger than the original pore content without regularity. Therefore, combined with the results of the two experiments, it can be found that when water +$CO_2$ adsorption is 144 hours, the pore content of 2~12nm and >700nm is generally increased, and the pore content of 12~700nm is generally decreased, and the increase of $CO_2$ adsorption pressure has no regularity in the pore size distribution.

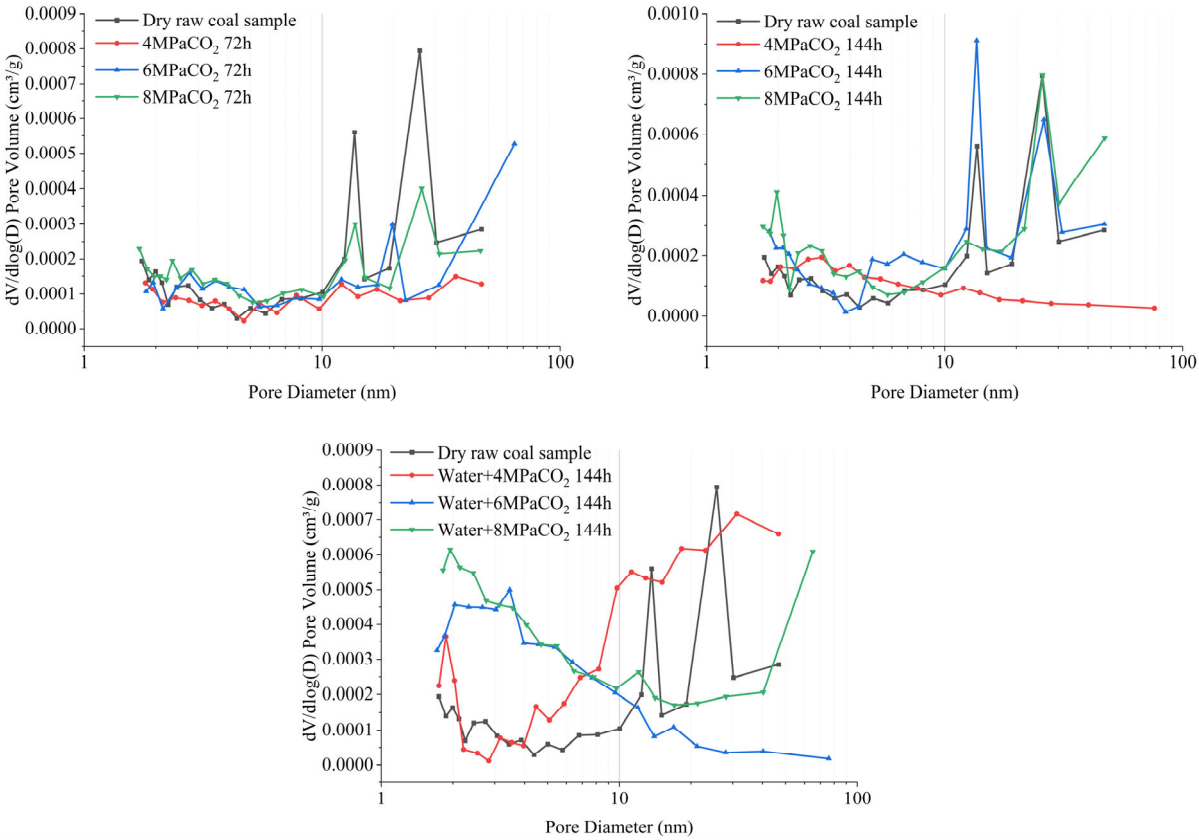


**Figure 1.** Pore size distribution of low temperature liquid nitrogen test of coal samples under different $CO_2$ adsorption pressures

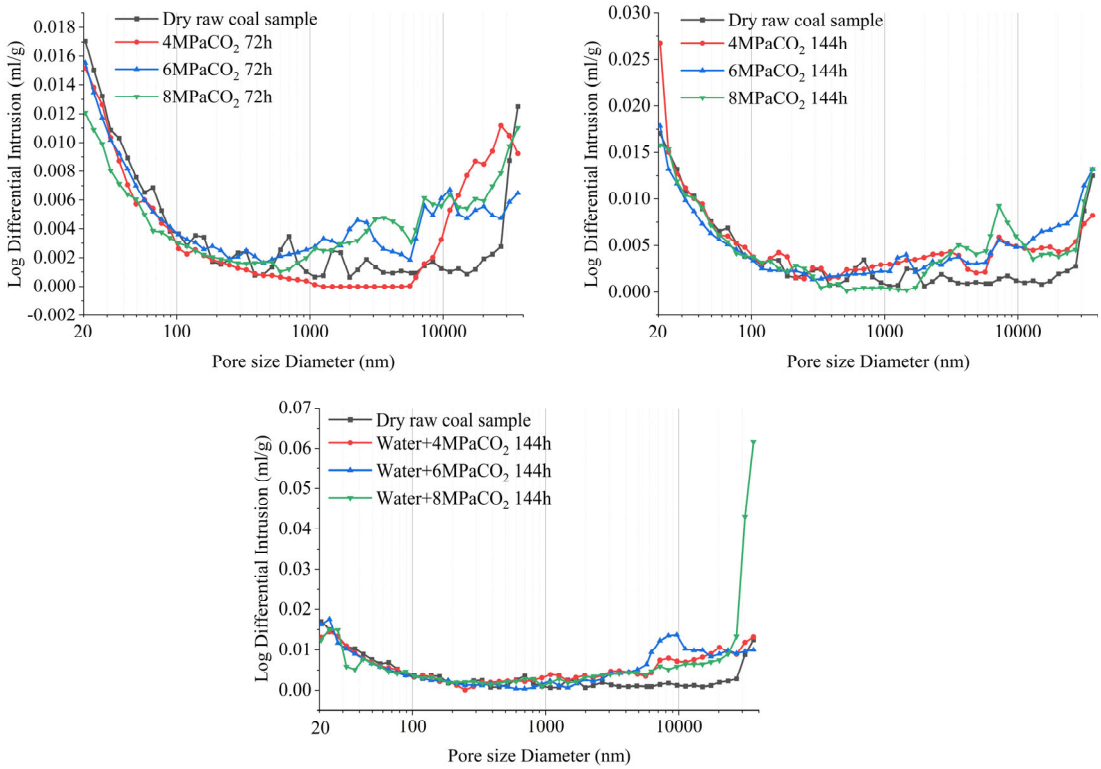


**Figure 2.** Pore size distribution of coal samples under high pressure mercury injection test under different $CO_2$ adsorption pressures

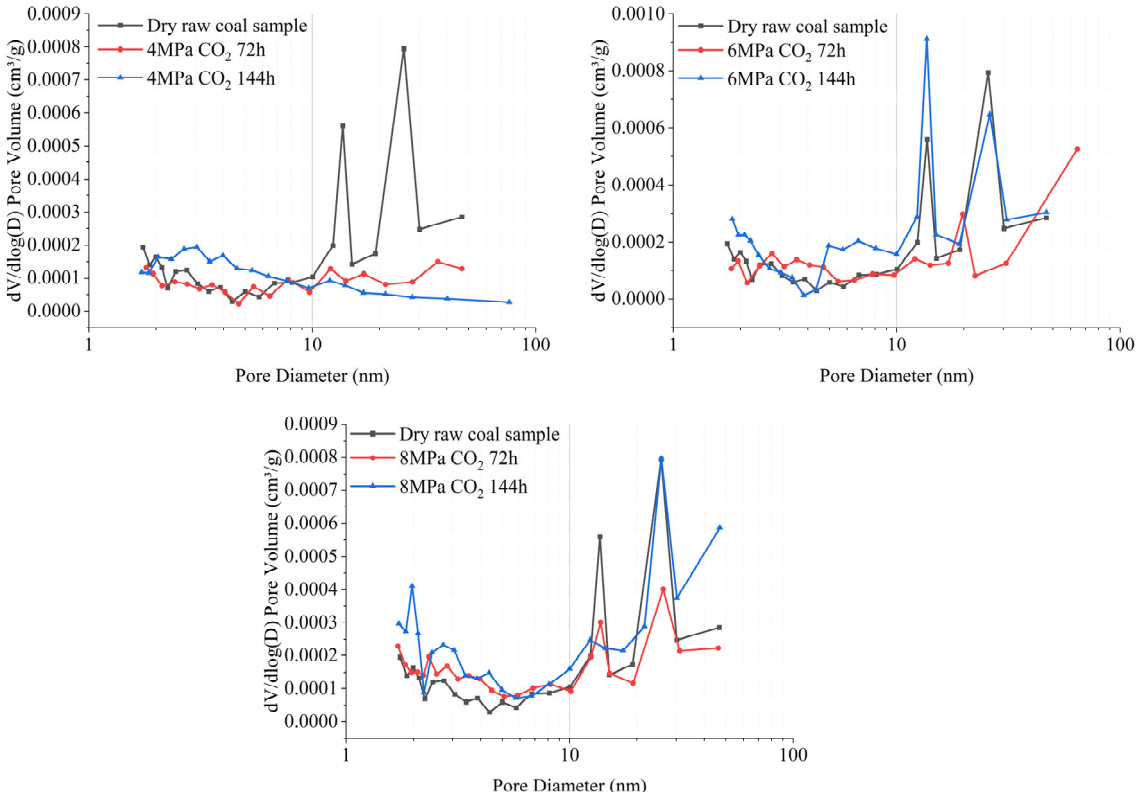


**Fig. 3** Pore size distribution of low temperature liquid nitrogen test of coal sample under different $CO_2$ adsorption time

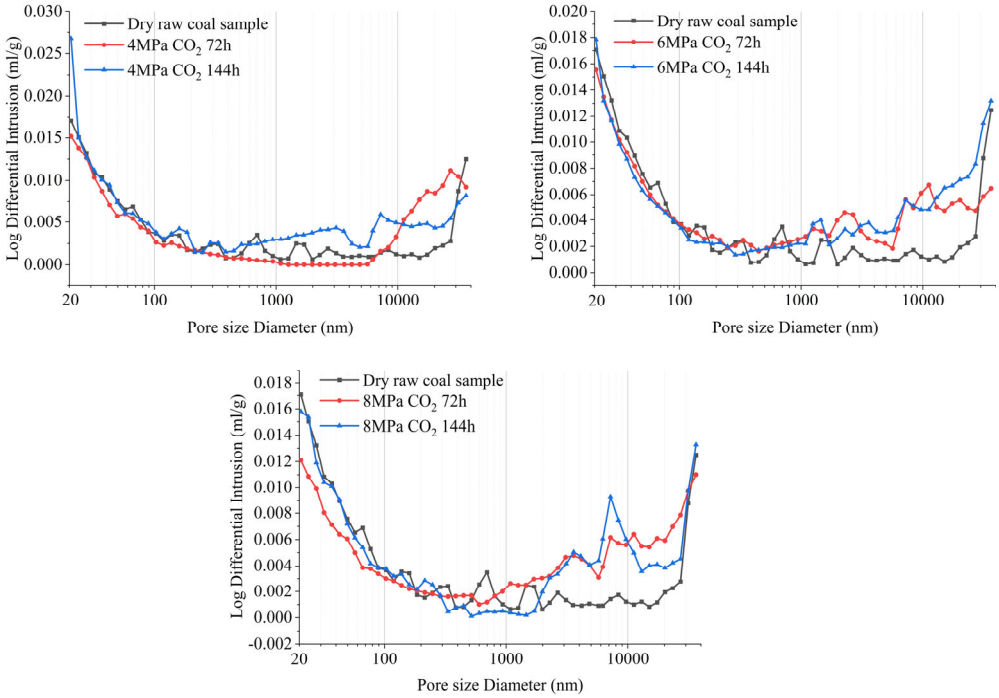


**Fig. 4** Pore size distribution of coal samples under high pressure mercury injection test at different $CO_2$ adsorption times

The pore size distribution results obtained by the low-temperature liquid nitrogen adsorption test and the high-pressure mercury injection test of the coal sample under different $CO_2$ adsorption pressures are shown in Fig. 3 and Fig. 4. It can be seen from the pore size distribution diagram of low-temperature nitrogen test that under the 4 MPa $CO_2$ adsorption condition, the pore content of coal sample between 2 and 8nm is generally greater than that of the original sample, and the pore content of coal sample between 8 and 50nm is significantly reduced. It can be seen from the pore size distribution diagram of high-pressure mercury injection test that under the 4 MPa $CO_2$ adsorption condition, the pore content of coal samples between 20 and 80nm decreases, the pore content of coal samples between 80 and 8000nm shows no regularity, and the pore content of coal samples >8000nm increases. Therefore, combined with the results of the two experiments, it can be found that in the case of 4 MPa $CO_2$ adsorption, the pore content of coal samples from 2~8nm and >8000nm increases, the pore content of coal samples from 8~80nm decreases, and the pore content of coal samples from 80~8000nm changes irregularly. Moreover, the prolongation of $CO_2$ adsorption time has no regularity in pore size distribution. It can be seen from the pore size distribution diagram of low-temperature nitrogen test that under the 6 MPa $CO_2$ adsorption condition, the pore content of coal sample between 2 and 11nm is generally greater than that of the original sample, and the pore content of coal sample between 11 and 50nm is reduced. It can be seen from the pore size distribution diagram of high pressure mercury injection test that the pore content of coal samples between 20 and 333nm decreases when $CO_2$ is adsorbed at 6 MPa, while the pore content of coal samples >333nm increases significantly. Therefore, combined with the results of the two experiments, it can be found that at 6 MPa $CO_2$ adsorption, pore content of coal samples from 2~11nm and >333nm increases, while pore content of coal samples from 11~333nm decreases, and the extension of $CO_2$ adsorption time has no regularity in pore size distribution. It can be seen from the pore size distribution diagram of low-temperature nitrogen test that under the adsorption of 8 MPa $CO_2$, the pore content between 2 and 11nm increases, while the pore content between 11 and 50nm decreases slightly. However, it can be seen from the pore size distribution diagram of high-pressure mercury injection test that under the adsorption of 8 MPa $CO_2$, the pore content between 20 and 385nm decreases, while the pore content of >385nm increases significantly. Therefore, combined with the results of the two experiments, it can be found that at 8 MPa $CO_2$ adsorption, the pore content of 2~11nm and >385nm increases, while

the pore content of 11~385nm decreases, and the pore size distribution is still not regular with the extension of $CO_2$ adsorption time.

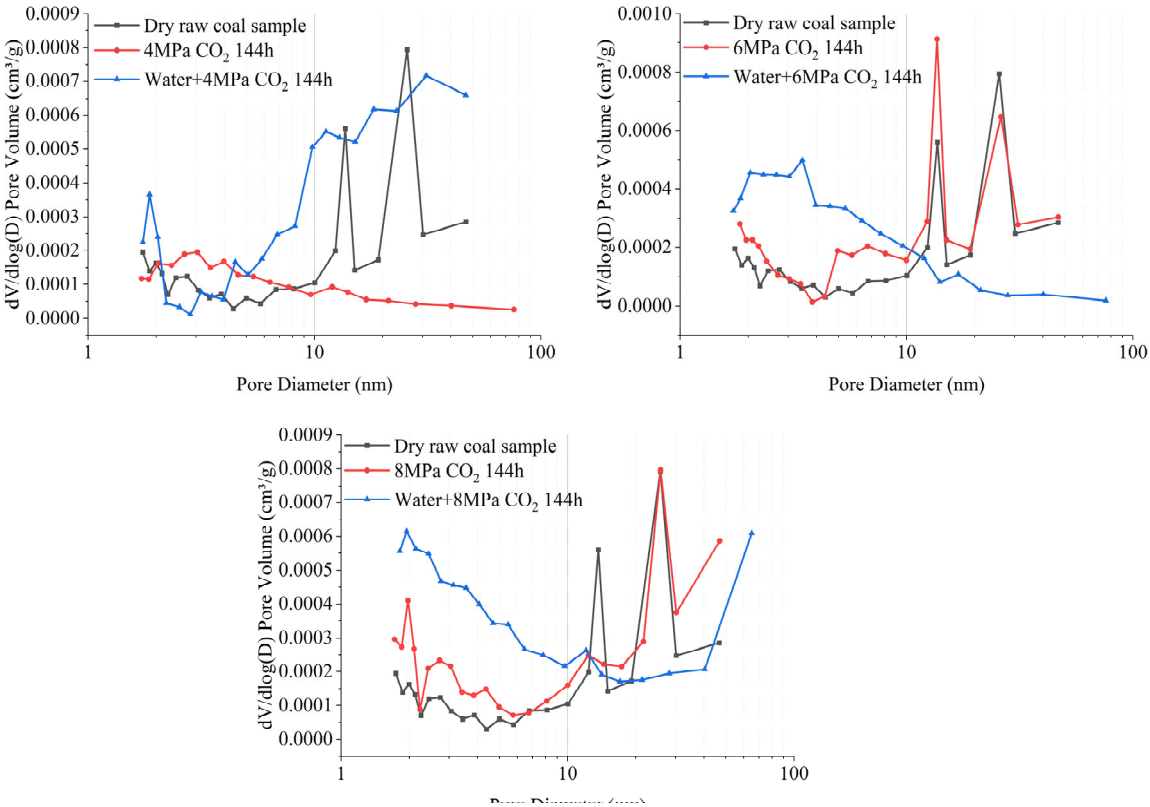


**Figure 5.** Pore size distribution of dry and wet coal samples tested by low temperature liquid nitrogen

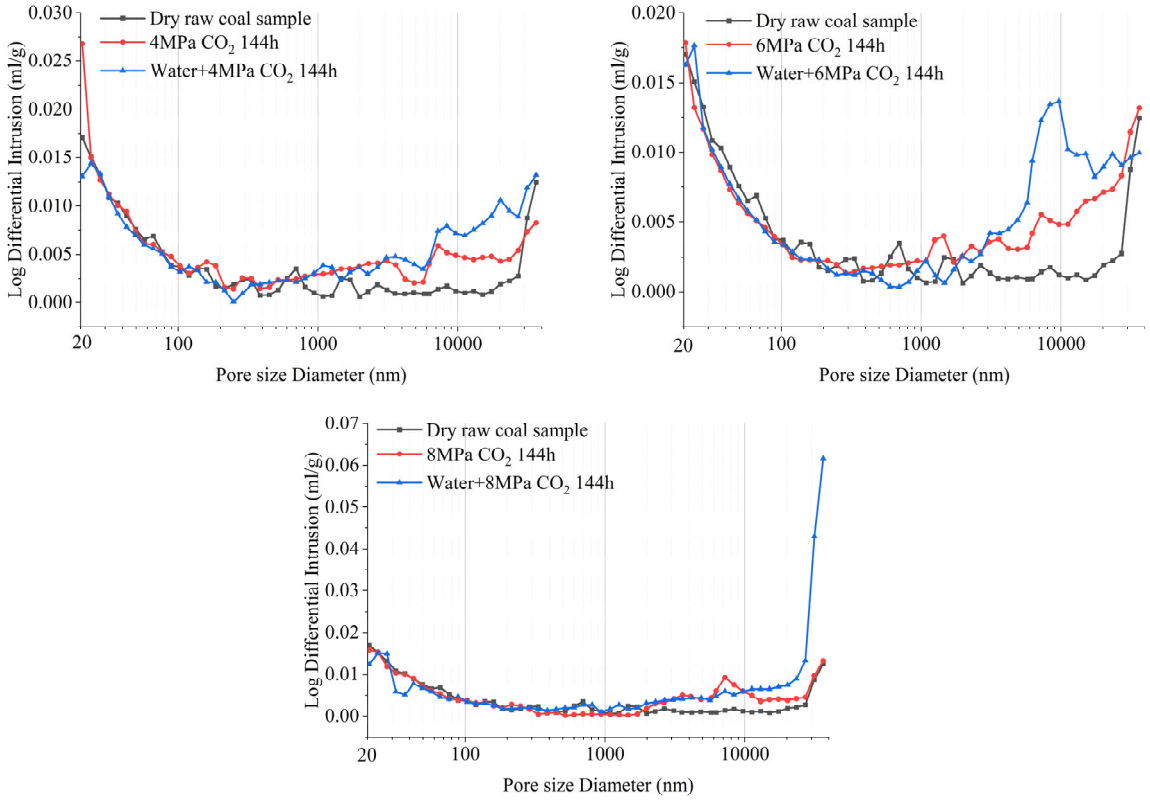


**Figure 6.** Pore size distribution of dry and wet coal samples under high pressure mercury injection test

The pore size distribution results obtained from the low temperature liquid nitrogen adsorption test of dry and wet coal samples and the high pressure mercury injection test are shown in Fig. 5 and Fig. 6. It can be seen from the pore diameter distribution diagram of low-temperature nitrogen test that the pore diameter changes did not show a rule after the intervention of water. The specific changes have been analyzed in Figure 3-4, and will not be repeated here. It can be seen from the pore size distribution map of high-pressure mercury injection test that the pore content of wet coal samples starts to increase significantly after 10μm, and the pore content is still irregular when the pore size is less than 10μm. Therefore, combined with the results of the two experiments, it can be found that the intervention of water has a significant positive effect on the increase of pore content of coal samples before 10μm, and has a significant positive effect on the increase of pore content after 10μm.

## 3.2. Pore connectivity change characteristics of coal

The mercury intake and withdrawal curves are shown in Figure 7. It can be seen from the figure that the mercury intake and mercury withdrawal curves of the samples treated with $CO_2$-$H_2O$ are basically higher than those of the dry raw coal samples regardless of prolonged $CO_2$ adsorption time, increased $CO_2$ adsorption pressure or increased $CO_2$-$H_2O$ treatment, indicating that the mercury intake and pore volume of the coal samples after the reaction increase, which is consistent with the analytical structure described above.

The inlet and outlet curves of mercury injection experiment generally have the characteristics of "pore hysteresis loop", and the basic morphology and connectivity of pores can be preliminatively evaluated according to the width of the pore hysteresis loop and the volume difference between inlet and outlet of mercury. It was first discovered by Ritter et al., and explained by the "inkpot hole" theory proposed by Mcbain. At present, there are mainly two theories to explain it. Some scholars believe that the delayed loop is formed by the change of the contact Angle between mercury and coal surface during the stage of mercury injection and mercury withdrawal. Some other scholars attributed the existence of the mercury delay ring to the connectivity and development characteristics of pores and fractures in coal. 1998 This theory is also a continuation of the "inkpot theory". When mercury is injected, the actual pore diameter is greater than or equal to the theoretical pore diameter value under the corresponding mercury injection pressure, and the pore interior is in a connected state, mercury can enter the pore interior, and when the pressure is able to fill all the space inside the pore, the pore is filled with mercury. During mercury withdrawal, when the path to the coal surface is no longer continuous, part of mercury will remain in the pore interior or the path to the coal surface. In particular, the pore shape in coal is complex, the width of the pores and their connecting channels is variable, and some pores have small entry channels. After mercury is injected into the pores, mercury cannot be completely withdrawn at the stage of mercury withdrawal due to the small channels and the contact Angle between mercury and the coal surface. Resulting in the stagnation of mercury in the pore, formed into mercury mercury withdrawal hysteresis loop, therefore, into the mercury mercury withdrawal hysteresis loop to a certain extent can characterize pore fracture network connected state, namely connectivity features. Scholars believe that the narrower the lag ring of mercury intake and mercury withdrawal, the better the connectivity of the test sample, that is, the closer the amount of mercury withdrawal is to the amount of mercury intake, indicating that the proportion of effective connected hole cracks in coal is higher.

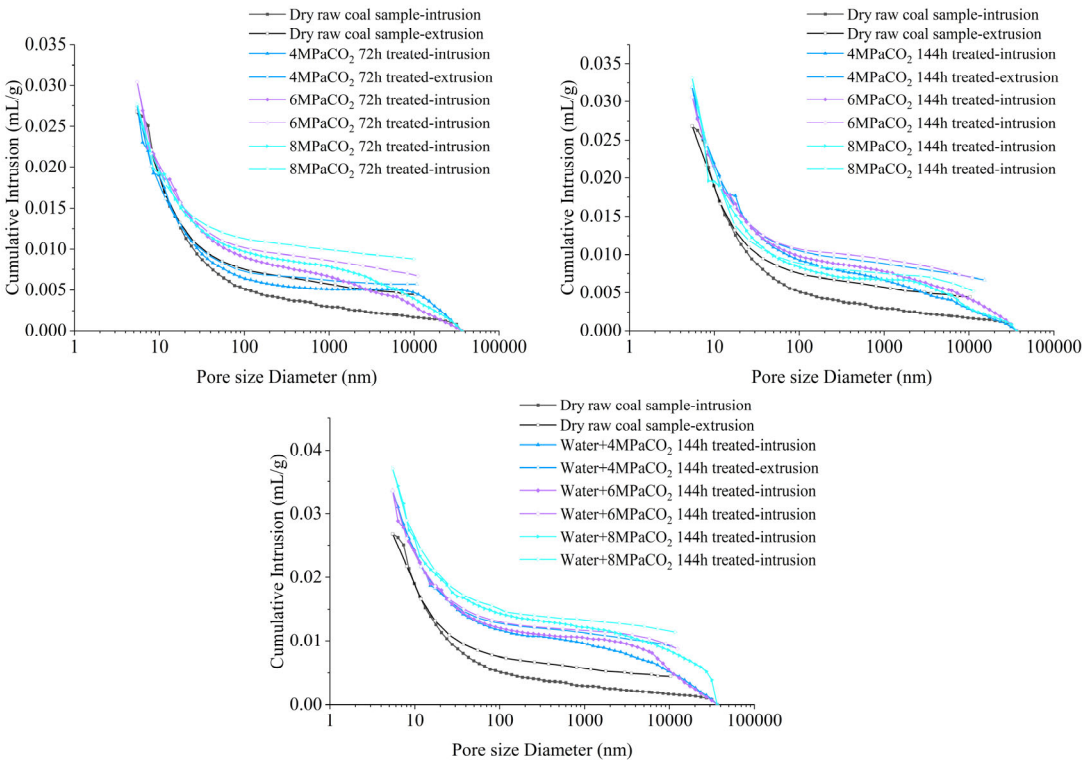


**Figure 7.** Hg intake and Hg withdrawal curves under different reaction conditions

In order to more accurately analyze the characteristics of pore connectivity changes before and after sample reaction, mercury removal efficiency can be used for analysis. In general, the higher the mercury removal efficiency, the better the connectivity of the pore system of the sample. It is defined as the ratio of the volume of mercury removed from the sample at the lowest pressure to the volume injected before lowering the pressure. The formula is:

$$W_e = \left(\frac{V_{max} - V_r}{V_{max}}\right) \times 100\% \quad (1)$$

Where $W_e$ is mercury extraction efficiency, $V_{max}$ is the volume of mercury injected under maximum pressure, and $V_r$ is the residual volume of mercury under minimum pressure.

**Table 3.** Mercury removal efficiency before and after coal sample reaction

| Number | Condition | $W_e$(%) |
|---|---|---|
| 1 | - | 83.38% |
| 2 | 4 MPa $CO_2$ 72h | 79.15% |
| 3 | 6 MPa $CO_2$ 72h | 78.06% |
| 4 | 8 MPa $CO_2$ 72h | 68.17% |
| 5 | 4 MPa $CO_2$ 144h | 79.11% |
| 6 | 6 MPa $CO_2$ 144h | 77.39% |
| 7 | 8 MPa $CO_2$ 144h | 84.25% |
| 8 | Water+4 MPa $CO_2$ 144h | 72.96% |
| 9 | Water+6 MPa $CO_2$ 144h | 74.04% |
| 10 | Water+8 MPa $CO_2$ 144h | 69.28% |

As can be seen from Fig. 7, coal samples show a certain mercury withdrawal lag before and after $CO_2$ action, which indicates that there are certain ineffective pores in coal. According to the mercury removal efficiency calculated in Table 3, only the mercury removal efficiency of the coal sample after 144 hours of adsorption of 8 MPa $CO_2$ is slightly higher than that of the dry sample, which indicates that $CO_2$ has a negative impact on the connectivity of the coal sample. In the above mercury injection test, pore volume of coal samples increased after $CO_2$ action, indicating that a large number of non-effectively connected pores were generated after $CO_2$ action. That is, $CO_2$ does increase a large number of pores in coal, but the pores are mainly non-connected pores, that is, $CO_2$ has a weak improvement in the connectivity of the pores in coal.

## 4. CONCLUSIONS

(1) The adsorption of $CO_2$ changes the pore content in coal. After $CO_2$ adsorption, pore content in coal shows a trend of first increasing, then decreasing and then increasing. $CO_2$ adsorption pressure, $CO_2$ adsorption time and $CO_2$-$H_2O$ slightly change the variation range of pore size, but the trend remains unchanged. For example, in the case of $CO_2$ adsorption for 72 hours, the pore content of 2~10nm and >700nm is generally increased, and the pore content of 10~700nm is significantly reduced. In the case of 144 hours of $CO_2$ adsorption, the pore content of 2~20nm and >700nm generally increased, and the pore content of 20~700nm significantly decreased. When water +$CO_2$ was adsorbed for 144 hours, the pore content of 2~12nm and >700nm generally increased, and the pore content of 12~700nm generally decreased.

(2) The coal samples showed a certain lag of mercury withdrawal before and after $CO_2$ action, which indicates that there are certain ineffective pores in the coal. The mercury removal efficiency of the coal sample after $CO_2$ adsorption is generally lower than that of the dry original sample, and the pore volume of the coal sample in the above mercury injection test increases after $CO_2$ action, indicating that a large number of non-effective connected pores are generated after $CO_2$ action. That is, $CO_2$ does increase a large number of pores in coal, but the pores are mainly non-connected pores, that is, $CO_2$ has a weak improvement in the connectivity of the pores in coal.

## REFERENCES


[1] Yao B, Wu Y, Liu J. The Effect of the Fracture Distribution On $CO_2$ Injection Into a Coal Seam. International Journal of Mining Science and Technology, 2012, 22(1):115-120.

[2] Cnudde V, Masschaele B, Dierick M, Vlassenbroeck J, Van Hoorebeke L, Jacobs P. Recent Progress in X-Ray Ct as a Geosciences Tool. Applied Geochemistry, 2006, 21(5):826-832.

[3] Ketcham R A, Iturrino G J. Nondestructive High-Resolution Visualization and Measurement of Anisotropic Effective Porosity in Complex Lithologies Using High-Resolution X-Ray Computed Tomography. Journal of Hydrology, 2005, 302(1-4):92-106.

[4] Mazumder S, Wolf K, Elewaut K, Ephraim R. Application of X-Ray Computed Tomography for Analyzing Cleat Spacing and Cleat Aperture in Coal Samples. International Journal of Coal Geology, 2006, 68(3-4):205-222.

[5] Karacan C O, Okandan E. Adsorption and Gas Transport in Coal Microstructure: Investigation and Evaluation by Quantitative X-Ray Ct Imaging. Fuel, 2001, 80(4):509-520.

[6] Dun W, Guijian L, Ruoyu S, Shancheng C. Influences of Magmatic Intrusion On the Macromolecular and Pore Structures of Coal: Evidences From Raman Spectroscopy and Atomic Force Microscopy. Fuel, 2014, 119:191-201.